

Structural Behavior of Self-Compacting Bendable Mortar Beams reinforced by GFRP Bars under Monotonic Loads

Tabark Mohammed

Department of Civil Engineering, College of Engineering, Mustansiriyah University, Baghdad, Iraq
tabark97@uomustansiriyah.edu.iq (corresponding author)

Wissam Alsaraj

Department of Civil Engineering, College of Engineering, Mustansiriyah University, Baghdad, Iraq
wkaswkas5@gmail.com

Luma A. Zghair

Department of Civil Engineering, College of Engineering, Mustansiriyah University, Baghdad, Iraq
drlumacivileng@uomustansiriyah.edu.iq

Received: 13 August 2024 | Revised: 14 September 2024 | Accepted: 19 September 2024

Licensed under a CC-BY 4.0 license | Copyright (c) by the authors | DOI: <https://doi.org/10.48084/etasr.8729>

ABSTRACT

Flexible or bendable concrete is an Engineered Cementitious Composite (ECC) that exhibits ductile material properties, in contrast to the brittle nature of conventional concrete. The material composition of conventional concrete is modified in order to impart a flexible nature to the material. This research presents the findings of an experimental study examining the flexural response of self-compacting bendable concrete beams reinforced by Glass Fiber Reinforced Polymers (GFRP) bars under a symmetrical two-point load. The experimental work comprised the casting of eight reinforced beams. The dimensions of all beams were identical: an overall height of 150 mm, a width of 100 mm, and a total length of 1,000 mm. The beams were classified into three groups based on the type of variables adopted and the type of the strengthening method employed, the percentage of steel fibers (1%, 1.5%, and 2%), and the percentage of Polyvinyl Alcohol (PVA) (0.2%, 0.3%, and 0.4%) were also considered. The following measurements were taken: the first cracking load, midspan vertical deflections, concrete surface strains, and the ultimate load capacity. Additionally, the crack patterns were recorded and the failure mode was observed, in addition to the mechanical properties of self-mortar bendable concrete (both fresh and hardened). The results indicated that an increase in the PVA ratio from 0.2% to 0.3% and 0.4% resulted in a notable rise in the modulus of rupture and modulus of elasticity, by approximately 16% and 40%, respectively, and 0.09% and 2%, respectively. The ductility of the beams increased with the steel fiber ratio due to enhanced flexural and splitting properties, which is a positive outcome. This allows for more caution to be exercised before the beam reaches its limit of stability. Furthermore, the value of deflection at maximum load increases with the increase of steel fiber content due to the increase in load capacity.

Keywords-bendable concrete; ECC; PVA; steel fiber; flexural behavior, GFRP; self-compacting

I. INTRODUCTION

Concrete is a building material that exhibits high compressive strength but low tensile strength. In the absence of reinforcement, a concrete beam will display cracking and failure when subjected to a relatively small load. The failure is typically abrupt and brittle in nature [1]. Flexible or bendable concrete is an Engineered Cementitious Composite (ECC) that demonstrates ductile material properties, which contrasts with the brittle nature observed in conventional concrete [2]. ECC has a tensile strain capacity of 5%, which is 500 times greater than that of plain concrete or Fiber-Reinforced Concrete (FRC)

[3]. The appealing for a multitude of applications nature of ECC emerges from the benefits of high composite ductility in the hardened state and flexible processing in the fresh state. A number of tests have been performed to evaluate the effectiveness of ECC at the structural level [3, 4]. These studies offer new insights into how the material characteristics influence the structure's responses. In order to predict the structural behavior, constitutive models of ECC have been developed and integrated into Finite Element (FEM) systems [5, 6]. Such studies should assist in investigating the selective application of ECC in key structural system components, while avoiding the need for costly experiments. The coarse aggregate

is eliminated in a flexible concrete mix, and more fibers are incorporated. Flexible concrete comprises cement, fibers, sand, water, and superplasticizer [7]. Bendable concrete is made of mortar rather than concrete, but with polymer addition, fiber is required to impart good workability. These different ingredients share the entire applied load [8]. It has been determined through empirical evidence that the integration of fibers into concrete can markedly augment its tensile strength, thereby reducing the likelihood of fissures forming in the concrete matrix [9-11]. The fibers present in the malleable concrete are equipped with an anti-friction coating, known as the slick coating. The coating enables the fibers to slide over one another, and does not result in the formation of friction between the fibers [12]. The robust molecular bond that is formed between the concrete and the fibers during the hydration process serves to prevent the occurrence of cracking. Furthermore, it exhibits self-healing properties, enabling the repair of microcracks. This results in increased concrete flexibility [13]. Bendable concrete exhibits a greater capacity for deformation than regular concrete while maintaining the incorporation of superfine silica sand and tiny PVA fibers. A mechanical strength test is conducted on the beam, which demonstrates the ability to withstand significant loads and deformations without the necessity for steel reinforcement. The flexural strength is 60% greater than that of the conventional concrete [14]. Steel fibers are currently the primary material used to reinforce concrete and resolve the issue of brittleness [15, 16].

The usage of fine sand for the purposes of water treatment represents an optimal approach for the production of flexible concrete. In the event that this is not available, it is possible to use normal sand as an alternative. Additionally, alternative materials, such as silica fume, blast furnace slag, and fly ash can be employed in the production of concrete [17]. The workability of flexible concrete is a requisite quality, and thus superplasticizers are a necessary component. The superplasticizers employed in the production of flexible concrete include lignin, naphthalene, melamine formaldehyde, sulphonate, polycarboxylate ether and lignosulfonates [18, 19]. An ECC represents a significant advancement in concrete technology, offering the potential to resist greater applied loads before cracking while behaving as a ductile material. This enhanced behavior can help to resist higher loads before failure and provide greater strength before collapse. An investigation into the behavior of reinforced concrete beams with GFRP bars under bending using ECC material will provide further insight into the behavior of bendable concrete. Glass Fiber-Reinforced Polymer (GFRP) is the most common substitute for steel bars in modern construction. The most significant benefit of GFRP bars is their high corrosion resistance, while possessing high tensile strength and low density, which makes them lightweight and exhibit excellent electromagnetic resistance [20-24]. They are frequently employed in wet and coastal regions to prolong the lifespan of concrete structures and curtail the costs associated with maintenance [25-27]. Given that steel bars have a greater mass than GFRP bars, incorporating steel into RC structures markedly increases the overall weight of the structure. Reducing the weight of buildings is of paramount importance. This highlights the necessity for the usage of

lighter building materials, which will prove beneficial for the overall functionality of the structures. The objective of this advanced study is to reduce the brittleness of concrete. It has been demonstrated in the literature that the addition of fibers to concrete enhances both the axial strength and flexibility of columns [28, 29]. GFRP bars are an effective means of providing interior reinforcement for concrete constructions, offering a number of advantageous mechanical and environmental resistance features [30, 31].

II. EXPERIMENTAL WORK

The objective of the experiment was to test how well supported beams can withstand a load in the middle, using a special type of concrete. To make sure the results were reliable, a series of tests were carried out on control specimens, including prisms, cylinders, and cubes.

A. Specimen Details

The eight beams were designed to display flexural failure and had identical dimensions. The total length of the beams was 1,000 mm, while the cross-sectional dimensions were (150x100) mm. The beams were divided into three groups based on the type of variables adopted, including the type of reinforcement (GFRP and steel bars), the volume fraction of steel fibers (SF) (1, 1.5% and 2%), and the percentage of PVA (0.2%, 0.3%, and 0.4%). These variables are presented in Table I and Figure 1, which also shows the dimensions and reinforcement details of the tested beams.

TABLE I. DETAILS OF TESTED BEAMS

Groups	Beam No.	PVA %	Steel Fiber %	P GFRP	Ps
A	B1	0.2	1	0.022	0
	B2	0.2	1.5	0.022	0
	B3	0.2	2	0.022	0
	B4	0.2	1	0.0146	0.0072
B	B5	0.2	1	0.0073	0.0144
	B6	0.2	1	0	0.0216
C	B7	0.3	1	0.022	0
	B8	0.4	1	0.022	0

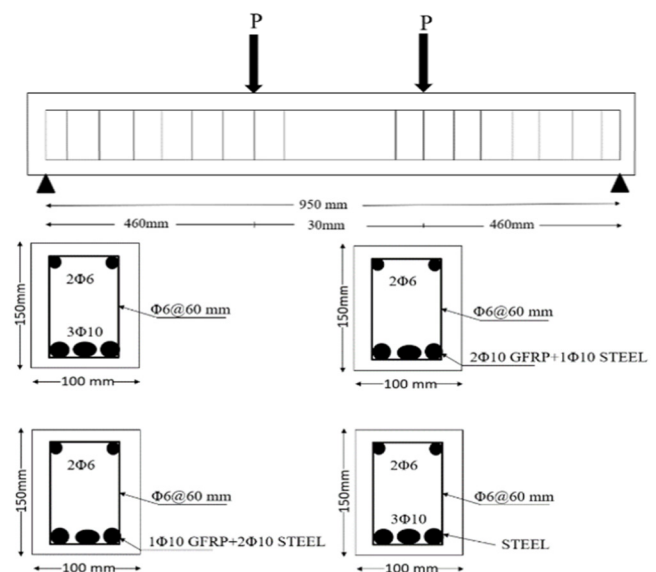


Fig. 1. Beam reinforcement details.

B. Materials

a) Materials of SECC and Mix Properties

The materials of the SECC mixture are ordinary Portland cement (CEM1-42.5 R), which is in compliance with the specifications set forth in Iraqi Regulation No. 5/2019 [32]. Tables II and III present the chemical and physical properties of the cement. The fine aggregate in question is a grade with a maximum size of 600 μm , and it is in compliance with Iraqi specifications requirement 45/2021 [33]. The grading zone of the fine aggregate has been determined to be zone 3, based on the findings of the relevant tests. The fineness of silica fume is 880 cm^2/gm , which is in accordance with the ASTM C1240/2005 requirements [34]. Additionally, micro steel fibers with lengths from 12 mm to 14 mm, diameters from 0.2 mm to 0.25 mm [35], and tensile strengths exceeding 2,850 MPa [36-38], were used. A liquid high-performance GLENIUM 51 ether-based superplasticizer was employed to mitigate the loss of workability. This plasticizer is categorized as type A and F in accordance with the classification system outlined in ASTM C494 [39]. The lengths of the PVA fibers used in the study ranged from 8 mm to 12 mm, with a diameter of 40 μm [40, 41]. A series of trial mixes were performed to ascertain the optimal superplasticizer dosage for enhancing workability, as determined by the slump flow test, which yielded a range of 24 mm to 26 mm [42, 43]. Additionally, the objective was to achieve a cubic compressive strength exceeding 30 MPa at 28 days. Table IV presents the final quantities of the materials utilized to prepare SECC per m^3 for the various mixes employed in this study. The proportion of steel fibers and PVA was maintained at a constant level across all trial mixes. Ultimately, trial Mix No. 4 and No. 5 were found to be

successful. However, Mix No. 5 was selected for further analysis due to its superior compressive strength at 28 days.

TABLE II. CHEMICAL COMPOSITION AND MAIN COMPOUNDS OF THE CEMENT

Chemical composition	Weight%	Iraqi Specifications No. 5/2019
SiO ₂	21.92	-
CaO	62.52	-
MgO	3.35	Not more than 5 %
Al ₂ O ₃	4.0	-
Fe ₂ O ₃	3.3	-
SO ₃	2.2	Less than 2.8 %
C ₃ A	5.02	More than 3.5 %
Loss on Ignition (LOI)	2.65	Not more than 4 %
Insoluble Residue (IR)	0.95	Less than 1.5 %
Lime Saturation Factor	0.71	0.66-1.02

TABLE III. PHYSICAL PROPERTIES OF CEMENT

Physical properties			
Name	Unit	No. 1	Iraqi Specification No. 5/2019
Specific Surface Area	cm^2/g	2,680	Not Less Than 2300
Initial Setting Time	min	160	Not Less Than 45
Final Setting Time	Hours	6.4	Not more than 10
Compressive strength at 2 days	MPa	27.0	Not Less Than 20
Compressive strength at 28 days	MPa	49.8	Not Less Than 42.5
Soundness by Autoclave Method	%	0.64	Not more than 0.8

In order to achieve the objectives of this study, five mixes based on the mix design method (EFNARC 2002) [42] were divided into two groups according to the type of variables adopted. These included different percentages of steel fiber (1%, 1.5%, and 2%) and the percentage of PVA (0.2%, 0.3%, and 0.4%). The results of these mixes are outlined in Table V.

TABLE IV. DETAILS OF TRIAL MIXES FOR SECC

No. Mix	Cement (kg/m ³)	Sand (kg/m ³)	Limestone (kg/m ³)	Steel fiber %	PVA %	Super Plasticizer (L/m ³)	Water (L/m ³)	Slump test (mm)	Compressive strength (MPa)
M1	400	1,375	100	1	0.2	12	242	18	---
M2	400	1,375	100	1	0.2	15	242	20	---
M3	400	600	200	1	0.2	10	150	22	---
M4	400	650	250	1	0.2	10	150	24	31
M5	400	650	250	1	0.2	10	150	24	42

TABLE V. DETAILS OF CONCRETE MIXES

No. Mix	Cement (kg/m ³)	Fine aggregate (kg/m ³)	Silica fume %	PVA %	Steel Fiber %	Limestone (kg/m ³)	Super Plasticizer (L/m ³)	Water (L/m ³)
M1	400	650	250	1	0.2	10	150	24
M2	400	650	10	0.2	1.5	250	10	150
M3	400	650	10	0.2	2	250	10	150
M4	400	650	10	0.3	1	250	10	150
M5	400	650	10	0.4	1	250	10	150

b) Reinforcement Beams

Deformed steel bars with a diameter of 10 mm [44, 45], are used in the tension zone to provide p (0.0072, 0.0144, 0.0216) for four beams and GFRP bars [46]. In comparison, 6 mm diameter reinforcement is employed in the compression zone to maintain the stability of the stirrups.

c) Test Measurements and Instrumentation

All beams were subjected to an applied four-point load (300 mm between loads) in order to subject the larger area of the

beam to a maximum moment, in accordance with the relevant standard. The hydraulic universal testing machine (MFL system) was employed to test all beam specimens with a maximum load capacity of 3000 kN, as shown in Figure 2. The recorded data included the first crack load, ultimate load, and deflection. Three mechanical dial gauges were deployed for the measurement of deflection, with an accuracy of 0.01 mm. One gauge was positioned centrally on the beam, while the other was affixed beneath the point loads, as portrayed in Figure 2.



Fig. 2. The details for the machine test.

III. EXPERIMENTAL RESULTS AND DISCUSSION

A. Fresh Concrete Properties

The tests were performed immediately after mixing to examine the filling ability, passing ability, and segregation resistance of fresh SECC. The results were found to align with the EFNARC [42] limitations for slump flow diameter (greater than or equal to 24 mm) and flow time range (7 to 7.5 seconds on average for all mixes), as depicted in Table VI.

TABLE VI. FRESH SECC TEST RESULTS

No.	Method	Property	Result	EFNARC Requirements
1	Slump flow	Filling ability	24	24-26
2	V-Funnel test	Filling & segregation resistance	7.5	7-11

B. Mechanical Properties of Hardened Concrete

a) Effect of Steel Fiber Ratio

The mechanical properties of the hardened concrete for group A are listed in Table VII. The results represented compressive strength f_{cu} [47], modulus of rupture f_r [48], splitting tensile strength f_t [49], and modulus of elasticity EC [50], as evidenced in Figures 3 and 4.

TABLE VII. MECHANICAL PROPERTIES OF EFFECT OF STEEL FIBER RATIO

Mix	Steel Fiber %	f_{cu} MPa	%	f'_c MPa	%	f_t MPa	%	f_r MPa	%	EC GPa	%
M1	1	42.34	---	35.08	---	6.05	---	7.75	---	27,837	---
M2	1.5	43.52	3	36.58	4	7.52	20	9.13	15	28,426	2
M3	2	46.24	8	38.54	9	9.55	36	11.57	33	29,178	5

The steel fibers exhibited high tensile and compressive strength and modulus of elasticity, which effectively impeded the propagation of microcracks within the matrix and enhanced the strength of the concrete.

b) PVA Ratio Content

The mechanical properties of the hardened concrete for Group B are presented in Table VIII. The results are expressed in terms of compressive strength f_{cu} , modulus of rupture f_r , splitting tensile strength f_t , and modulus of elasticity EC , as noted in Figures 5 and 6. The enhancement in the mechanical properties can be ascribed to the optimal bonding effect of the steel and PVA fibers, which was predicated on the uniform

distribution of the fibers within the matrix. The hybridization of fiber reinforcement can facilitate further improvements in the mechanical behavior of composites. This is achieved by controlling the spread of cracks at variable stages of deformation and enhancing the strength of the concrete.

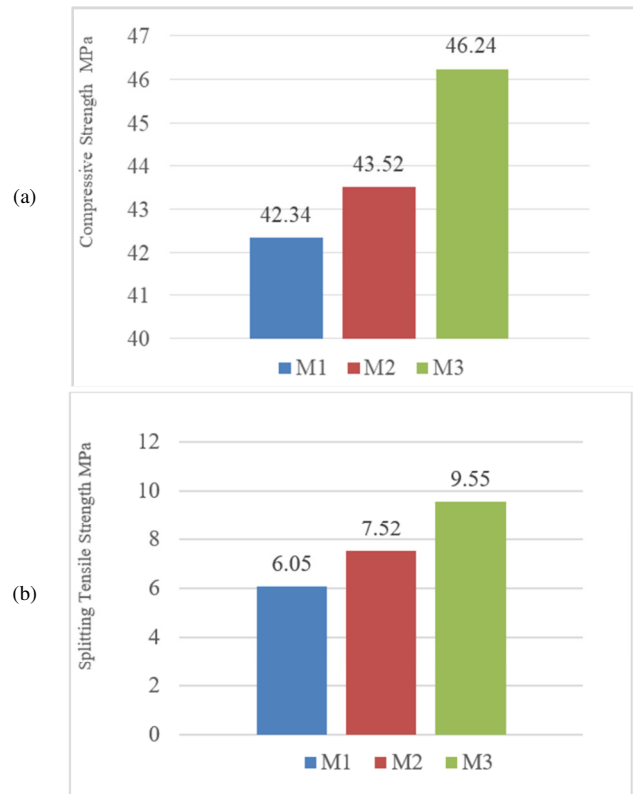


Fig. 3. (a) Compressive strength and (b) splitting tensile strength of the effect of steel fiber ratio.

TABLE VIII. MECHANICAL PROPERTIES OF PVA RATIO CONTENT

Mix	M1	M4	M5
PVA %	0.2	0.3	0.4
f_{cu} (MPa)	42.34	43.11	44.25
%	---	2	4
f'_c (MPa)	35.08	35.14	36.75
%	---	0.2	4
f_t (MPa)	7.75	6.92	8.1
%	---	13	25
f_r (MPa)	7.75	9.25	13.75
%	---	16	40
EC (GPa)	27,837	27,861	28,422
%	---	0.09	2

C. Flexural Behavior of SECC

The load capacity and deflection of eight concrete beams tested up to failure under symmetrical two-point loads were employed in a study of their flexural behavior.

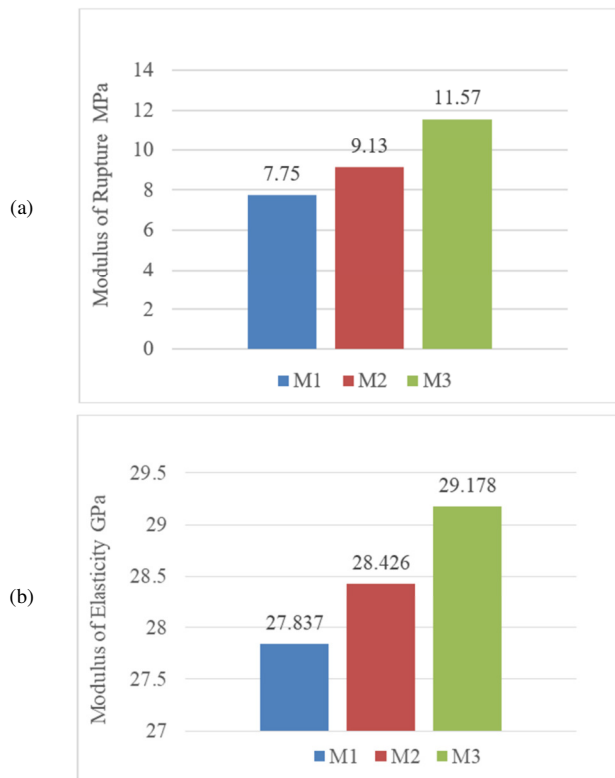


Fig. 4. (a) Modulus of rupture and (b) modulus of elasticity of the effect of steel fiber ratio.

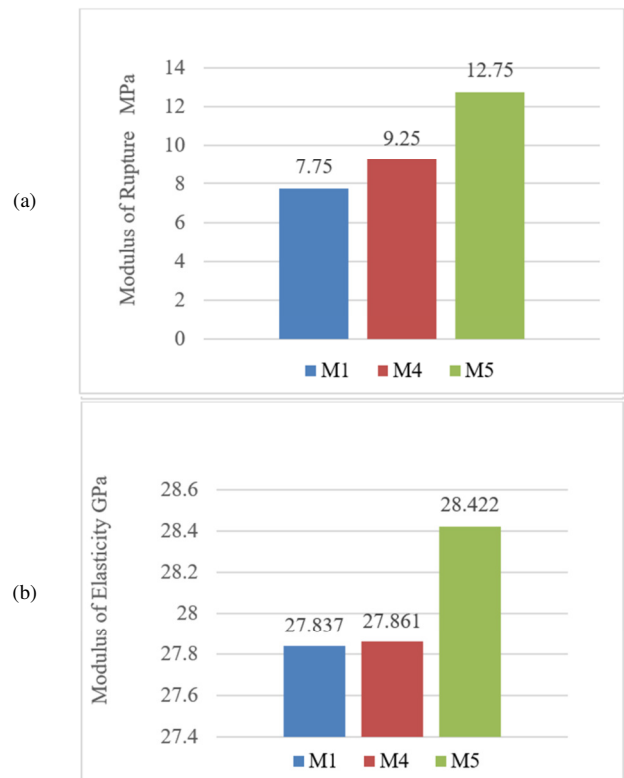


Fig. 6. (a) Modulus of rupture and (b) modulus of elasticity of PVA ratio content.

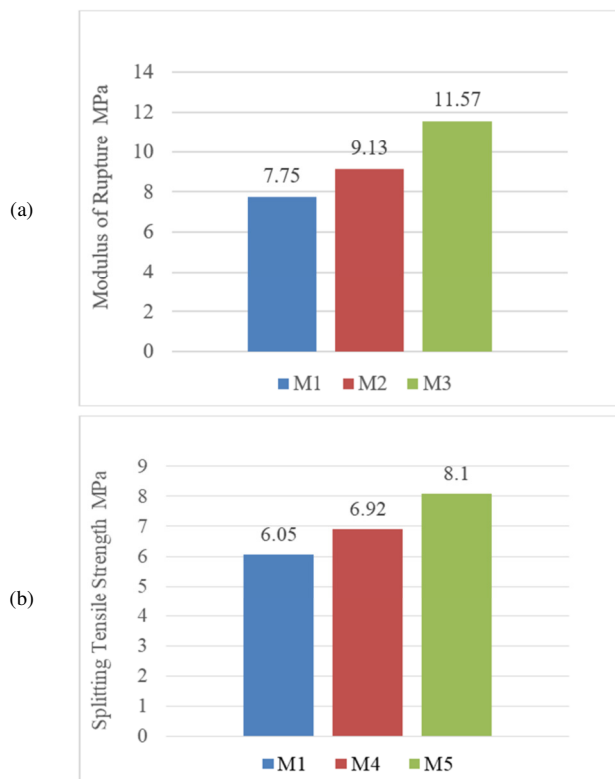


Fig. 5. (a) Compressive strength and (b) splitting tensile strength of PVA ratio content.

a) Group A: Effect of Steel Fiber Ratio

The group comprises three beams, designated B1, B2, and B3. All variables remain constant in this group, with the exception of the percentage of SF, which varies from 1 to 1.5 and 2 for B1, B2, and B3, respectively. Table IX provides the experimental results of group A.

TABLE IX. EXPERIMENTAL RESULTS OF GROUP A

Group A		Silica=10%		PVA=0.2%		GFRP=0.022	
Beams	Steel fiber %	f_{cr} kN	%	P_u kN	%	Ultimate deflection mm	%
B1	1	40	---	130	---	15.5	---
B2	1.5	44	10	145	10	17	9
B3	2	47	15	155	16	19	18

An increase in the steel fiber ratio from 1% to 1.5% and 0.2% resulted in a notable rise in the first crack load by approximately 10% and 15%, respectively, and in the ultimate load by approximately 10% and 16%. As the steel fiber ratio increases from 1% to 1.5% and 2%, the corresponding deflection value at ultimate load also increases, reaching values of approximately 9% and 18%, respectively, as shown in Figures 7 and 8, presenting the enhanced ductility of beams with an increase in the steel fiber ratio, attributable to augmented flexural and splitting properties. This is a beneficial outcome, as it allows for more cautious monitoring of the structure. Additionally, the deflection value at maximum load rises in conjunction with the rise in the steel fiber content, reflecting the growth in load capacity.

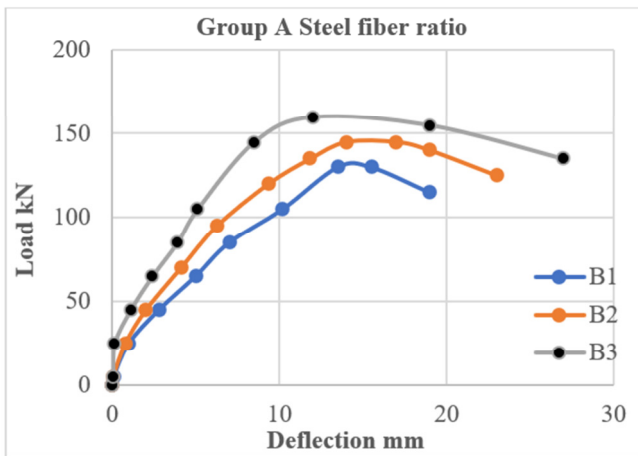


Fig. 7. Load-deflection curve of beam for group A.

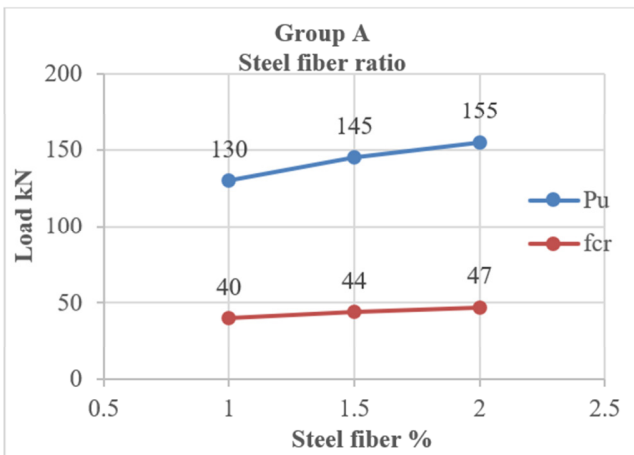


Fig. 8. Experimental results of Group A.

b) Group B: Type Reinforcement Effect

This group comprises the type and reinforcement value for four beams, B1, B4, B5, and B6. Two types of reinforcement are employed in this group: GFRP bars with $\rho = 0.022, 0.0146, 0.0073,$ and $0,$ and steel bars with $\rho = 0, 0.0072, 0.0144,$ and $0.0216,$ respectively. These are used to investigate the influence of the reinforcement on the behavior of beams. As evidenced by the data presented in Table X and Figures 9 and 10, a reduction in the P (GFRP) from 0.022 to 0.0146 and an increase in the P (Steel) from 0 to 0.0072 resulted in an increase in the first crack, ultimate loads, and deflection corresponding to ultimate loads. The values for the first crack, ultimate loads, and deflection increased by approximately 11%, 19%, and 18%, respectively. Additionally, a decrease in P (GFRP) from 0.022 to 0.0073 and an increase in P (Steel) from 0 to 0.0144 led to a 20% and 24% increase, respectively, in the values of the first crack and ultimate loads. Conversely, the deflection decreased by approximately 29%. A decrease in P (GFRP) from 0.022 to 0, accompanied by an increase in P (Steel) from 0 to 0.0216, resulted in a 25%, 28%, and 43% increase in the values of the first crack and ultimate loads, respectively. This behavior indicates that the steel

reinforcement should remain in place until the GFRP bars have gradually reached their maximum strength. The enhanced ductility properties and modulus of elasticity enabled the beams to reach their ultimate strength before failure, thereby increasing their capacity.

TABLE X. EXPERIMENTAL RESULTS OF GROUP B

Beams	Group B		Silica=10%		PVA=0.2%		Steel Fiber=1 %	
	P GFRP	P Steel	f_{cr} kN	%	P_u kN	%	Ultimate deflection mm	%
B1	0.022	0	40	---	130	---	15.5	---
B4	0.0146	0.0072	45	11	160	19	19	18
B5	0.0073	0.0144	50	20	170	24	12	-29
B6	0	0.0216	53	25	185	28	27.36	3

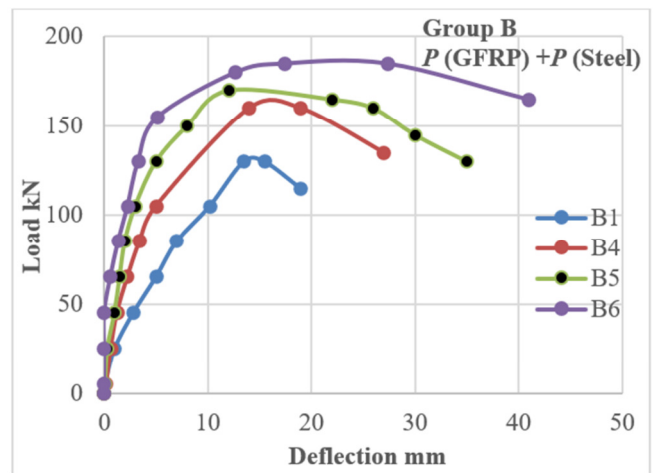


Fig. 9. Load-deflection curve of group B.

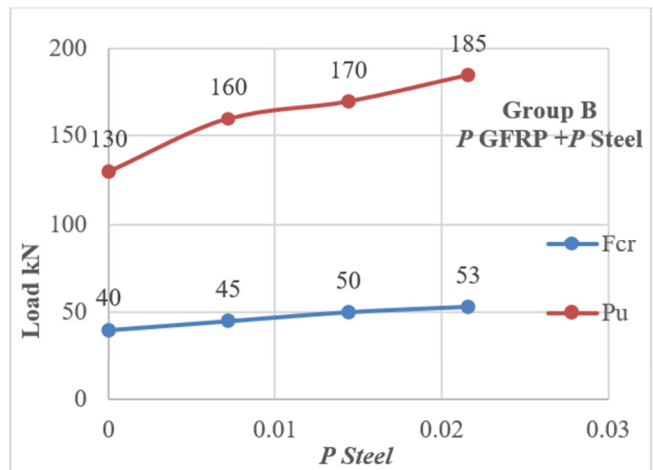


Fig. 10. Experimental results of group B.

c) Group C: Effect of PVA Ratio

The group consisted of three beams, designated B1, B7, and B8. All variables were held constant in Group C, with the exception of the value of the PVA ratio, which was 0.2%, 0.3%, and 0.4% for B1, B7, and B8, respectively. Table XI shows the ultimate load, first crack load, and deflection of

Group C. An increase in the PVA ratio from 0.2% to 0.3% and 0.4% resulted in a notable rise in the first crack load by approximately 11% and 27%, respectively, and in the ultimate load by approximately 8% and 15%, respectively. As the PVA ratio increases from 0.2% to 0.3% and 0.4%, the deflection value corresponding to the ultimate load demonstrates an increase of approximately 26% and 44%, respectively, as presented in Figures 11 and 12. This behavior can be attributed to an enhancement in the ductility of the concrete due to the rise in PVA content. The incorporation of PVA fibers delays the initial formation of cracks and reduces their width, while this enables the beam to withstand greater loads before reaching its limit and failing.

TABLE XI. EXPERIMENTAL RESULTS OF GROUP C

Group C		Steel Fiber =1%		Silica=10%		P (GFRP)=0.022	
Beams	PVA %	f_{cr} kN	%	P_u kN	%	Ultimate deflection mm	%
B1	0.2	40	---	130	---	15.5	---
B7	0.3	45	11	141	8	21	26
B8	0.4	55	27	153	15	28	44

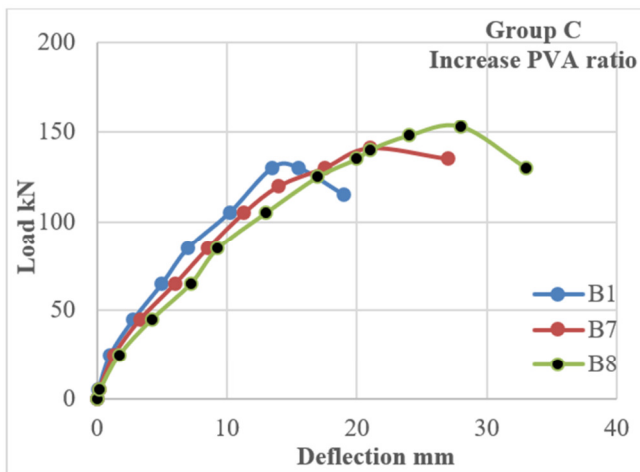


Fig. 11. Load-deflection curve of group C.

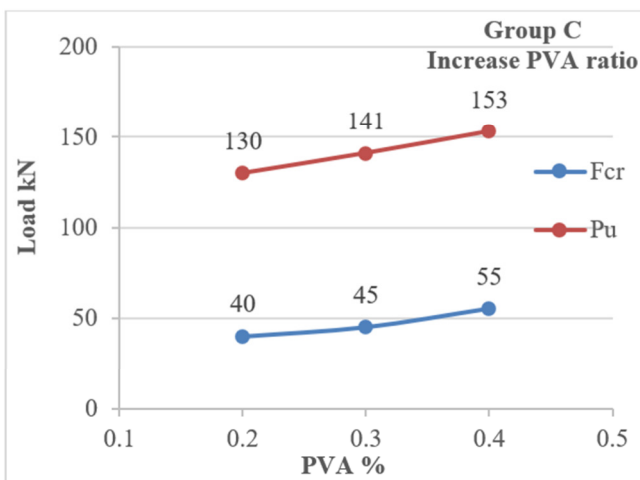


Fig. 12. Experimental results of group C.

D. Cracked Pattern and Mode of Failure

The results obtained for the cracking load and crack pattern for all beams are depicted in Figure 13. Crack patterns emerged at locations where tensile stresses (in specific points) surpassed the specified concrete tensile strength. During the testing process, a multitude of micro flexural cracks appeared in regions of critical importance due to the tensile stresses exerted by flexural forces. As the load increased, the cracks extended and widened. It was observed that the initial cracking phenomenon occurred at a later stage in the SECC samples in comparison to the normal concrete, which was attributed to the incorporation of steel fibers and PVA.

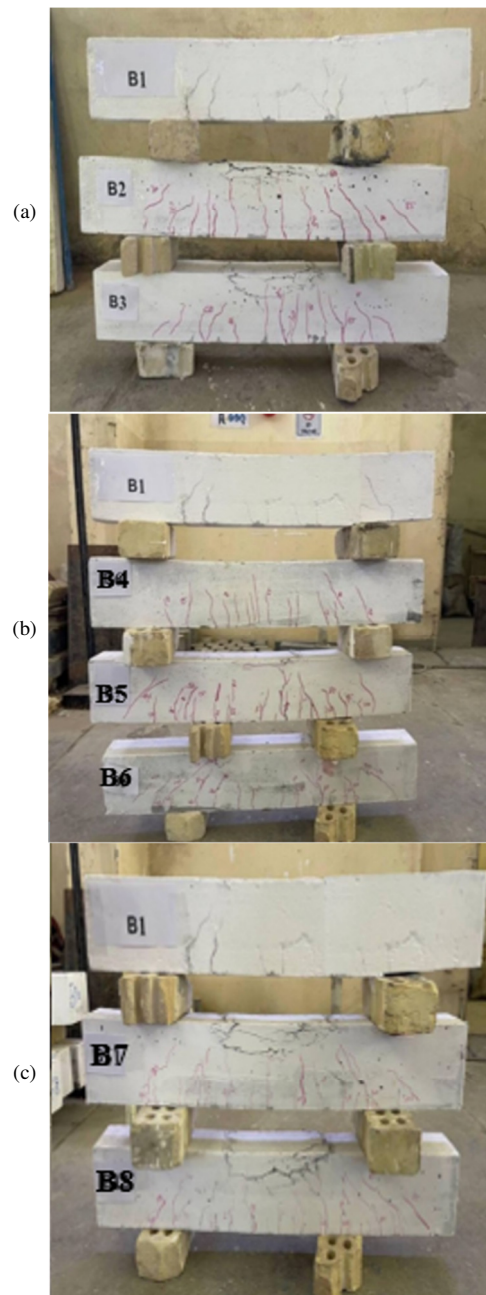


Fig. 13. Crack pattern for all beams, (a) B2, B3, (b) B4, B5, B6, (c) B7, B8.

An increase in the percentage of steel fibers resulted in a delay in the initial appearance of cracks in all SECC beams, as observed in the beam designated "B1," which represents the minimum steel percentage. Additionally, it is evident that flexural cracks have formed beneath the loaded points, which are described as vertical and passing through the neutral axes of the beams. It was noted that an increase in the percentage of PVA resulted in a notable increase in the number of cracks in bendable concrete, which led to a delay in the formation of cracks or an increase in their width, thus delaying failure. Furthermore, it was observed that an increase in the percentage of iron fibers had a significant impact on the durability of the beams. This was due to the transfer of stress from the cracked areas to the intact regions, which prevented the extension of cracks towards the loading point.

E. Ductility Index

Ductility is a characteristic that demonstrates the capacity of RC beams to undergo plastic deformation before reaching failure while maintaining a significant portion of their flexural strength [51], as illustrated in Table XII. Figure 14, shows how the ductility of SECC beams is enhanced when the quantity of steel tension reinforcement within the beam is augmented in hybrid reinforcement beams. In comparison to the reference beams, the SECC beams with a PVA content of 0.4% exhibited a 163% improvement in ductility.

TABLE XII. DUCTILITY INDEX FOR ALL BEAMS

Beam No.	Variables.	Δy (mm)	Δu (mm)	Ductility Index	
				$\Delta u/\Delta y$	%
B1	$S.F = 1\%$	4.9	19	3.8	--
B2	$S.F = 1.5\%$	5.8	23	3.9	3
B3	$S.F = 2\%$	5.6	27	4.8	26
B4	$P_g = 0.0146 + P_s = 0.0072$	4.2	27	4.4	16
B5	$P_g = 0.0073 + P_s = 0.0144$	5.2	35	6.7	76
B6	$P_g = 0 + P_s = 0.0216$	3.5	41	11.7	208
B7	PVA=0.3%	4.1	27	6.5	71
B8	PVA=0.4%	3.3	33	10	163

F. Flexural Toughness

The flexural toughness of concrete is defined as a measure of the capacity of the material to absorb energy. Additionally, it is employed to quantify the resistance of concrete to cracking and ductility. The toughness values were determined for all the beams examined by calculating the area under the curve using Excel software and AutoCAD 2022. Table XIII presents the flexural toughness for all casted reinforcement beams. The flexural toughness of the SECC beams with GFRP bar reinforcement and 2% steel fiber content (B3) was evidenced to exhibit a markedly higher value than that of other beams. The observed increase in flexural toughness may be attributed to two factors: increased deflection and enhanced energy absorption.

G. Flexural Stiffness

The flexural stiffness of a structural member is regarded as one of its primary characteristics. The capacity of a body to resist deformation under the influence of an applied force is quantified by an index known as its degree of deformation

resistance. The initial stiffness is defined as the gradient of the linear segment observed in the load-deflection curve prior to the occurrence of the first flexural fracture.

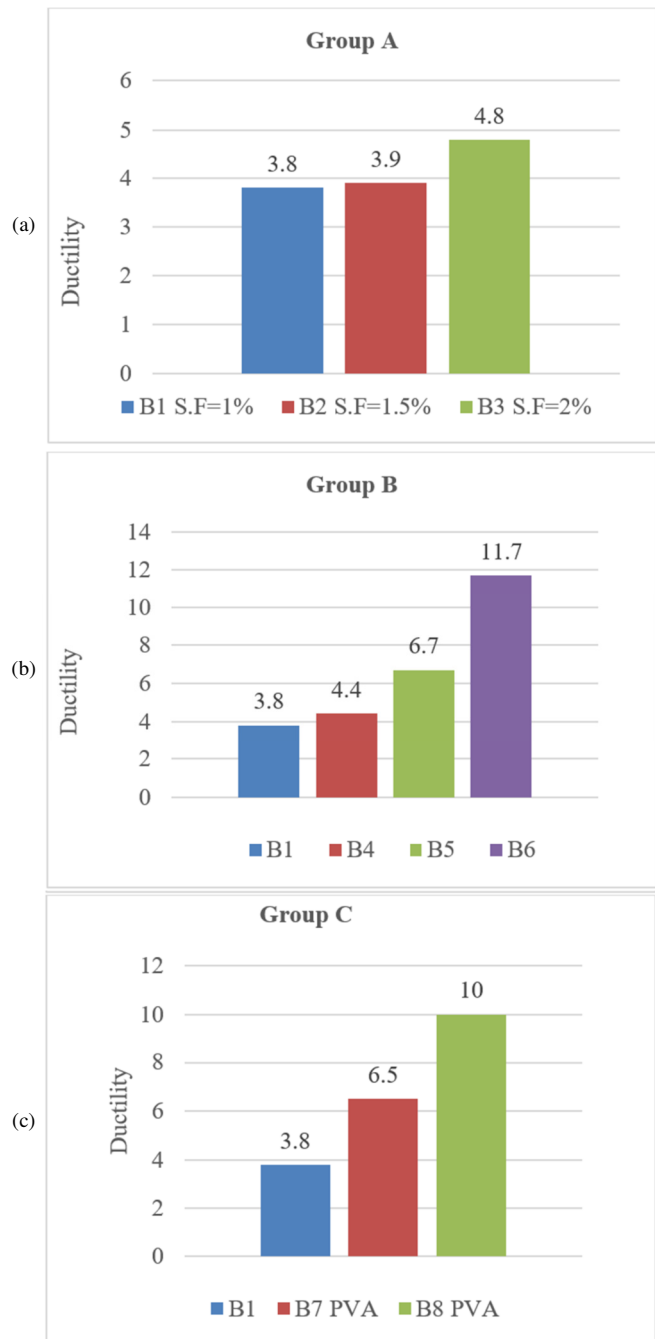


Fig. 14. Ductility index for groups (a) A, (b) B, and (c) C.

Table XIV portrays the stiffness values for all tested beams. It is proposed that enhancing the reinforcement ratio could potentially improve the initial stiffness of the specimen while reducing the occurrence of folds. A comparison of the SECC beams with one another under monotonic load revealed a notable increase in stiffness with an increase in the number of

longitudinal reinforcement steel bars. The initial stiffness and service stiffness increased by 89% and 70%, respectively, with an increase in the percentage of reinforcement bars.

TABLE XIII. FLEXURAL TOUGHNESS FOR ALL BEAMS

Beam No.	Variables	Strain Energy kN.mm
B1	$S.F = 1\%$	159
B2	$S.F = 1.5\%$	261
B3	$S.F = 2\%$	524
B4	$P_g = 0.0146 + P_s = 0.0072$	205
B5	$P_g = 0.0073 + P_s = 0.0144$	286
B6	$P_g = 0 + P_s = 0.0216$	273
B7	PVA = 0.3%	182
B8	PVA = 0.4%	255

IV. CONCLUSIONS

The discussions of the results obtained are summarized as follows:

- The successful acquisition of bendable, self-compacting concrete is of critical importance for the concreting of areas with dense reinforcement or challenging to compact conditions.
- The usage of bendable and self-compacting concrete confers a substantial advantage in terms of postponing failure. This is due to the fact that the constituents of this concrete assist in the prevention of the rapid formation of cracks, thereby enhancing its capacity to withstand increased loading.
- The incorporation of Polyvinyl Alcohol (PVA) fibers into concrete has proven to enhance numerous mechanical properties, particularly those related to tensile strength. The addition of these fibers increases the concrete's capacity to withstand applied loads before reaching failure, a phenomenon attributed to the enhanced tensile properties of the fibers themselves.
- As the PVA ratio increases from 0.2% to 0.3% and 0.4%, the value of the modulus of rupture and the modulus of elasticity demonstrates a notable increase, reaching approximately 16% and 40%, respectively, and 0.09% and 2%, respectively.
- The hybridization of fiber reinforcement can continue to enhance the mechanical behavior of composites by regulating the propagation of cracks at varying stages of deformation and augmenting the strength of the concrete.
- It was observed that the initial cracking phenomenon was delayed in the SECC samples due to the presence of steel fibers and PVA.
- It was noted that the structural behavior of SECC beams tends to be more flexible than that of SCC.
- In general, failure in SECC beams is safer than that in beams made of SCC, due to the very high deflection compared to ordinary concrete. Therefore, it may provide a greater opportunity for warning in the event of a failure.

TABLE XIV. STIFFNESS FOR ALL THE TESTED BEAMS

Beam No.	Variables	P_{cr} (kN)	Δ_{cr} (mm)	P_y (kN)	Δ_y (mm)	Intimal Stiffness		Service Stiffness	
						KN/mm	%	KN/mm	%
B1	$S.F = 1\%$	40	2	65	4.9	20	---	13.3	---
B2	$S.F = 1.5\%$	44	2	90	5.8	22	9	15.5	14
B3	$S.F = 2\%$	47	1.2	138	7.6	39.2	49	18.2	26
B4	$P_g = 0.0146 + P_s = 0.0072$	45	1.23	98	4.2	36.5	45	23.3	43
B5	$P_g = 0.0073 + P_s = 0.0144$	50	1.2	110	5.2	41.7	52	21.15	37
B6	$P_g = 0 + P_s = 0.0216$	53	0.3	156	3.5	177	89	44.5	70
B7	PVA=0.3%	45	3.3	76	4.1	13.6	-47	18.5	28
B8	PVA=0.4%	55	5.5	78	3.3	10	-100	23	42

ACKNOWLEDGMENTS

The authors are grateful for the financial support towards this research provided by the Civil Engineering Department, College of Engineering at Mustansiriyah University, Baghdad, Iraq.

REFERENCES

- [1] H. Nordin, "Fibre reinforced polymers in civil engineering: flexural strengthening of concrete structures with prestressed near surface mounted CFRP rods," M.S. thesis, Department of Civil, Environmental and Natural Resources Engineering, Lulea University of Technology, Lulea, Sweden, 2003.
- [2] W. Al-Juboori and L. Weekes, "A study of the shear behavior of CFRP strengthened beams incorporating a shear plane," Ph.D. dissertation, University of Salford, Salford, Manchester, UK, 2011.
- [3] V. C. Li, S. Wang, and C. Wu, "Tensile Strain-Hardening Behavior of Polyvinyl Alcohol Engineered Cementitious Composite (PVA-ECC)," *Materials Journal*, vol. 98, no. 6, pp. 483–492, Nov. 2001, <https://doi.org/10.14359/10851>.
- [4] G. Fischer, S. Wang, and V. C. Li, "Design of engineered cementitious composites (ECC) for processing and workability requirements," in *Brittle Matrix Composites 7*, 1st ed., A. M. Brandt, V. C. Li, and I. H. Marshall, Eds. Poland: Woodhead Publishing, 2003, pp. 29–36.
- [5] P. Kabele, *Assessment of structural performance of engineered cementitious composites by computer simulation*. Prague, Czech Republic: Czech Technical University, 2001.
- [6] T.-S. Han, P. H. Feenstra, and S. L. Billington, "Simulation of Highly Ductile Fiber-Reinforced Cement-Based Composite Components Under Cyclic Loading," *Structural Journal*, vol. 100, no. 6, pp. 749–757, Nov. 2003, <https://doi.org/10.14359/12841>.
- [7] V. C. Li, "Integrated structures and materials design," *Materials and Structures*, vol. 40, no. 4, pp. 387–396, May 2007, <https://doi.org/10.1617/s11527-006-9146-4>.

- [8] J. Zhou, S. Qian, G. Ye, O. Copuroglu, K. van Breugel, and V. C. Li, "Improved fiber distribution and mechanical properties of engineered cementitious composites by adjusting the mixing sequence," *Cement and Concrete Composites*, vol. 34, no. 3, pp. 342–348, Mar. 2012, <https://doi.org/10.1016/j.cemconcomp.2011.11.019>.
- [9] P. S. Song and S. Hwang, "Mechanical properties of high-strength steel fiber-reinforced concrete," *Construction and Building Materials*, vol. 18, no. 9, pp. 669–673, Nov. 2004, <https://doi.org/10.1016/j.conbuildmat.2004.04.027>.
- [10] W. H. Sultan, "Behavior of Steel Fibers Reinforced SCC Deep Beams under Shear Effect," Ph.D. dissertation, Civil Engineering Department, Al-Mustansiriyah University, Baghdad, Iraq, 2013.
- [11] S. M. Ali and H. K. Awad, "The Effect of Hybrid Fibers on Some Properties of Structural Lightweight Self-Compacting Concrete by using LECA as Partial Replacement of Coarse Aggregate," *Engineering, Technology & Applied Science Research*, vol. 14, no. 4, pp. 15002–15007, Aug. 2024, <https://doi.org/10.48084/etasr.7425>.
- [12] K. Selvakumar, R. K. Kumar, and A. Deivasigamani, "Experimental Study on the Properties of Bendable Concrete," in *International Conference on Recent Trends in Civil Engineering, Technology and Management (ICRTCEM)*, Virudhunagar, India, 2020.
- [13] P. Zhang and Q. Li, "Fracture Properties of Polypropylene Fiber Reinforced Concrete Containing Fly Ash and Silica Fume," *Research Journal of Applied Sciences, Engineering and Technology*, vol. 5, pp. 665–670, Jan. 2013, <https://doi.org/10.19026/rjaset.5.5006>.
- [14] Y. Zhu, Y. Yang, and Y. Yao, "Use of slag to improve mechanical properties of engineered cementitious composites (ECCs) with high volumes of fly ash," *Construction and Building Materials*, vol. 36, pp. 1076–1081, Nov. 2012, <https://doi.org/10.1016/j.conbuildmat.2012.04.031>.
- [15] L. A. Zghair, S. R. Al-Taa, and S. R. Abbas, "Preparation and Engineering properties of Slurry Infiltrated Fibrous Concrete (SIFCON)-A Review," *Al-Rafidain Journal of Engineering Sciences*, vol. 2, no. 1, pp. 322–329, 2024, <https://doi.org/10.61268/pp447670>.
- [16] L. Al-Jaberi, "The Influences of the Mineral Admixtures and Steel Fibers on the Fresh and Hardened Properties of SCC," M.S. thesis, Civil Engineering Department, Al-Mustansiriyah University, Baghdad, Iraq, 2005.
- [17] M. Singh, B. Saini, and H. D. Chalak, "Properties of Engineered Cementitious Composites: A Review," in *Proceedings of the 1st International Conference on Sustainable Waste Management through Design*, Ludhiana (Punjab), India, 2019, pp. 473–483, https://doi.org/10.1007/978-3-030-02707-0_54.
- [18] S. Gadhiya, T. N. Patel, and D. Shah, "Parametric Study on Flexural Strength of ECC," *IJSRD - International Journal for Scientific Research & Development*, vol. 3, no. 4, pp. 1494–1497, 2015.
- [19] J. Zhang, Z. Wang, and X. Ju, "Application of ductile fiber reinforced cementitious composite in jointless concrete pavements," *Composites Part B: Engineering*, vol. 50, pp. 224–231, Jul. 2013, <https://doi.org/10.1016/j.compositesb.2013.02.007>.
- [20] H. J. Zadeh and A. Nanni, "Design of RC Columns Using Glass FRP Reinforcement," *Journal of Composites for Construction*, vol. 17, no. 3, pp. 294–304, Jun. 2013, [https://doi.org/10.1061/\(ASCE\)CC.1943-5614.0000354](https://doi.org/10.1061/(ASCE)CC.1943-5614.0000354).
- [21] A. Raza, Q. Z. Khan, and A. Ahmad, "Numerical Investigation of Load-Carrying Capacity of GFRP-Reinforced Rectangular Concrete Members Using CDP Model in ABAQUS," *Advances in Civil Engineering*, vol. 2019, no. 1, 2019, Art. no. 1745341, <https://doi.org/10.1155/2019/1745341>.
- [22] M. Elchalakani, M. Dong, A. Karrech, M. S. Mohamed Ali, and J.-S. Huo, "Circular Concrete Columns and Beams Reinforced with GFRP Bars and Spirals under Axial, Eccentric, and Flexural Loading," *Journal of Composites for Construction*, vol. 24, no. 3, Jun. 2020, Art. no. 04020008, [https://doi.org/10.1061/\(ASCE\)CC.1943-5614.0001008](https://doi.org/10.1061/(ASCE)CC.1943-5614.0001008).
- [23] N. Elmessalami, A. El Refai, and F. Abed, "Fiber-reinforced polymers bars for compression reinforcement: A promising alternative to steel bars," *Construction and Building Materials*, vol. 209, pp. 725–737, Jun. 2019, <https://doi.org/10.1016/j.conbuildmat.2019.03.105>.
- [24] M. A. E. Zareef, "An Experimental and Numerical Analysis of the Flexural Performance of Lightweight Concrete Beams reinforced with GFRP Bars," *Engineering, Technology & Applied Science Research*, vol. 13, no. 3, pp. 10776–10780, Jun. 2023, <https://doi.org/10.48084/etasr.5871>.
- [25] B. Benmokrane, E. El-Salakawy, A. El-Ragaby, and T. Lackey, "Designing and Testing of Concrete Bridge Decks Reinforced with Glass FRP Bars," *Journal of Bridge Engineering*, vol. 11, no. 2, pp. 217–229, Mar. 2006, [https://doi.org/10.1061/\(ASCE\)1084-0702\(2006\)11:2\(217\)](https://doi.org/10.1061/(ASCE)1084-0702(2006)11:2(217)).
- [26] B. Benmokrane, E. El-Salakawy, S. El-Gamal, and S. Goulet, "Construction and Testing of an Innovative Concrete Bridge Deck Totally Reinforced with Glass FRP Bars: Val-Alain Bridge on Highway 20 East," *Journal of Bridge Engineering*, vol. 12, no. 5, pp. 632–645, Sep. 2007, [https://doi.org/10.1061/\(ASCE\)1084-0702\(2007\)12:5\(632\)](https://doi.org/10.1061/(ASCE)1084-0702(2007)12:5(632)).
- [27] O. S. AlAjarmeh, A. C. Manalo, B. Benmokrane, P. V. Vijay, W. Ferdous, and P. Mendis, "Novel testing and characterization of GFRP bars in compression," *Construction and Building Materials*, vol. 225, pp. 1112–1126, Nov. 2019, <https://doi.org/10.1016/j.conbuildmat.2019.07.280>.
- [28] A. Raza and Q. Z. Khan, "Experimental and numerical behavior of hybrid-fiber-reinforced concrete compression members under concentric loading," *SN Applied Sciences*, vol. 2, no. 4, Mar. 2020, Art. no. 701, <https://doi.org/10.1007/s42452-020-2461-5>.
- [29] P. Paultre, R. Eid, Y. Langlois, and Y. Lévesque, "Behavior of Steel Fiber-Reinforced High-Strength Concrete Columns under Uniaxial Compression," *Journal of Structural Engineering*, vol. 136, no. 10, pp. 1225–1235, Oct. 2010, [https://doi.org/10.1061/\(ASCE\)ST.1943-541X.0000211](https://doi.org/10.1061/(ASCE)ST.1943-541X.0000211).
- [30] F. Abed and A. R. Alhafiz, "Effect of basalt fibers on the flexural behavior of concrete beams reinforced with BFRP bars," *Composite Structures*, vol. 215, pp. 23–34, May 2019, <https://doi.org/10.1016/j.compstruct.2019.02.050>.
- [31] A. Manalo, B. Benmokrane, K.-T. Park, and D. Lutze, "Recent developments on FRP bars as internal reinforcement in concrete structures," *Concrete in Australia*, vol. 40, no. 2, pp. 46–56, Jan. 2014.
- [32] *IQS for Portland Cement*. Baghdad, Iraq: Central Organization for Standardization and Quality Control, 2019.
- [33] *IQS for Aggregates of Natural Resources used for Concrete and Construction*. Baghdad, Iraq: Central Organization for Standardization and Quality Control, 1984.
- [34] *Standard Specification for Use of Silica Fume for Use as a Mineral Admixture in Hydraulic-Cement Concrete, Mortar, and Grout*. West Conshohocken, PA, USA: ASTM International, 2003.
- [35] N. A. Memon, M. A. Memon, N. A. Lakho, F. A. Memon, M. A. Keerio, and A. N. Memon, "A Review on Self Compacting Concrete with Cementitious Materials and Fibers," *Engineering, Technology & Applied Science Research*, vol. 8, no. 3, pp. 2969–2974, Jun. 2018, <https://doi.org/10.48084/etasr.2006>.
- [36] W. Abbass, M. I. Khan, and S. Mourad, "Evaluation of mechanical properties of steel fiber reinforced concrete with different strengths of concrete," *Construction and Building Materials*, vol. 168, pp. 556–569, Apr. 2018, <https://doi.org/10.1016/j.conbuildmat.2018.02.164>.
- [37] A. Rana, "Some studies on steel fiber reinforced concrete," *International Journal of Emerging Technology and Advanced Engineering*, vol. 3, no. 1, pp. 120–127, Jan. 2013.
- [38] H. F. Naji, N. N. Khalid, W. K. Alsaraj, M. I. Haboub, and S. Marchetty, "Experimental investigation of flexural enhancement of RC beams with multi-walled carbon nanotubes," *Case Studies in Construction Materials*, vol. 14, Jun. 2021, Art. no. e00480, <https://doi.org/10.1016/j.cscm.2020.e00480>.
- [39] *Standard Specification for Chemical Admixtures for Concrete*. West Conshohocken, PA, USA: ASTM International, 1999.
- [40] D. T. C. Madhavi, L. Raju, and D. Mathur, "Polypropylene Fiber Reinforced Concrete-A Review," *International Journal of Emerging Technology and Advanced Engineering*, vol. 4, no. 4, pp. 114–119, Jun. 2014.

-
- [41] W. Zhenbo, Z. Jun, W. Jiahe, and S. Zhengjie, "Tensile performance of polyvinyl alcohol–steel hybrid fiber reinforced cementitious composite with impact of water to binder ratio," *Journal of Composite Materials*, vol. 49, no. 18, pp. 2169–2186, Aug. 2015, <https://doi.org/10.1177/0021998314542450>.
- [42] *Guidelines for Self-Compacting Concrete*. Farnham, UK: EFNARC, 2002.
- [43] *The European Guidelines for Self-Compacting Concrete Specification, Production and Use*. European Project Group, 2005.
- [44] *Standard Specification for Deformed and Plain Carbon-Steel Bars for Concrete Reinforcement*. West Conshohocken, PA, USA: ASTM International, 2009.
- [45] *Standard Test Methods and Definitions for Mechanical Testing of Steel Products*. West Conshohocken, PA, USA: ASTM International, 2013.
- [46] *Guide for designing and constructing structural concrete reinforced with fiber-reinforced polymer FRP bars*. Buffalo, NY, USA: ACI, 2015.
- [47] *Standard Test Method for Compressive Strength of Cylindrical Concrete Specimens*. West Conshohocken, PA, USA: ASTM International, 2021.
- [48] *Standard Test Method for Splitting Tensile Strength of Cylindrical Concrete Specimens*. West Conshohocken, PA, USA: ASTM International, 2017.
- [49] *Standard Test Method for Static Modulus of Elasticity and Poisson's Ratio of Concrete in Compression*. West Conshohocken, PA, USA: ASTM International, 2014.
- [50] *Standard Test Method for Flexural Strength of Concrete (Using Simple Beam with Third-Point Loading)*. West Conshohocken, PA, USA: ASTM International, 2003.
- [51] J. H. Ling, Y. T. Lim, and E. Jusli, "Methods to Determine Ductility of Structural Members: A Review," *Journal of the Civil Engineering Forum*, pp. 181–194, May 2023, <https://doi.org/10.22146/jcef.6631>.